Auto-adaptive and Dynamical Clustering for Open-Circuit Fault Diagnosis of Power Inverters

Thanh Hung Pham, Sanda Lefteriu, Cécile Labarre, Eric Duviella, Stéphane Lecoeuche

Auto-adaptive and Dynamical Clustering for Open-Circuit Fault Diagnosis of Power Inverters

Thanh Hung Pham, Sanda Lefteriu, Cécile Labarre, Eric Duviella, Stéphane Lecoeuche

***Abstract*— This paper presents a fault diagnosis approach for single open-circuit faults in inverters entirely from measurements of the stator currents. These measurements are used to extract the feature data; the feature data is then used to create clusters in an on-line, adaptive and unsupervised way. Auto-adaptive and Dynamical Clustering (AUDyC [1], [2]) is the algorithm employed for this step. Based on the derived clusters, appropriate formulations for the data labelling and fault detection and isolation are proposed. The effectiveness of the approach is validated on simulation and experiment data.**

I. Introduction

An inverter is a power converter that changes Direct Current (DC) to Alternative Current (AC). It is usually used to connect DC sources (e.g., battery) and AC electrical devices (e.g., AC electric motor). Fault diagnosis of the 3-phase inverter associated to a 3-phase motor represents an active area of research [3]. Because of aging or abnormal operating conditions, semiconductor switches, such as Insulated-Gate Bipolar Transistors (IGBTs), are the most vulnerable components in the inverter. Their failure is due to the Short-Circuit (SC) and Open-Circuit (OC) faults. The SC fault leads to a high current which is destructive and makes the system shut down immediately thanks to standard protection systems [4]. However, when the OC fault happens, the system can still run with degraded performance causing secondary faults on other system components. Thus, this paper focuses on OC fault diagnosis of 3-phase power inverters.

In terms of methodology, most researchers focus on one of these four approaches: model-based, signal-based, data-driven and hybrid [5]. The model-based approach uses the system model, obtained by physical principles or system identification techniques, to predict the output, which is compared to the measured output for diagnosing the fault [6]. It should be noted that this model is generally difficult to derive for a complex system, e.g., an asynchronous motor associated with an inverter. Instead of system models, the signal-based approach considers the measured signals for extracting features which are used, together with prior knowledge on the symptoms of healthy systems, to make diagnosis decisions [3], [7]. However, this approach does not take into consideration the dynamics of the input signal which is usually impacted by unknown disturbances or unbalanced conditions. In contrast to the two previous approaches, data-driven approaches consider a large volume of data and prior knowledge of considered systems to make fault diagnosis decisions thanks to data classification or clustering. Nevertheless, this approach suffers from a high computational cost, and may not identify unknown fault types. To combine the strengths of the previous approaches, our paper proposes a hybrid approach where signal-based and data-driven methods are combined.

For the 3-phase inverter, such a hybrid approach may be based on measurements of voltages and/or currents. Voltage-based methods use measurements of the three voltages at the inverter output [4]. This method is independent of the load, but requires additional sensors. The latter disadvantage motivates us to develop a current-based method, the load independence being ensured by simply normalizing the current data [3], [8].

The data-driven approach is used to determine the feature classes, which are feature vector sets characterizing system operation modes. In the context of OC fault diagnosis for inverters, previous works employed well-established statistical methods such as Principle Component Analysis (PCA) [4] and Support Vector Machines (SVM) [9], [10]. For these previous methods, reference classes are already available from the training data, and one needs to determine to which class the new feature vector belongs to. For this reason, they are called supervised methods, and unknown operation modes may not be detected during the actual system operation. To avoid this, Neural Networks (NN) can be applied to learn and diagnose the OC faults of inverters thanks to its powerful ability in non-linear approximation and adaptive learning [11]–[14]. However, in these papers, the number of classes is fixed, while the characteristics of the class is adapted to include the new feature vector. This issue may be tackled using adaptive unsupervised methods, where reference classes (called clusters) are not available a priori, but are created on-line. To our best knowledge, such a method has not to be applied to diagnose the OC fault of inverters yet. Moreover, most of existing clustering methods do not predict the time evolution of modelled data classes and their fusion.

In this paper, we employ the normalized DC current for the feature extraction, and Auto-adaptive and Dynamical Clustering (AUDyC) algorithm [1], [2] for feature clustering. AUDyC does on-line, adaptive and unsupervised feature learning, hence the unknown modes of operation can be learnt from the measurement data. The main contribution of our work resides in the application of AUDyC to perform

Thanh Hung Pham, Sanda Lefteriu, Cécile Labarre, Eric Duviella, Stéphane Lecoeuche are with Institut Mines Telecom Lille Douai, IA, F-59508 Douai, France {thanh-hung.pham, sanda.lefteriu, cecile.labarre, eric.duviella, stephane.lecoeuche} @imt-lille-douai.fr

single OC fault diagnosis of inverters by identifying representative data classes. Furthermore, appropriate conditions for labelling classes and for diagnosing faults are presented.

The paper is organized as follows. Section II formulates the fault diagnosis problem. Section III describes the proposed method, and section IV validates it on two test cases: the first considers simulation data from a 3-phase inverter, while the second is measurement data from a 5-phase inverter. Section V concludes the paper and presents future work directions.

II. The Inverter in Normal and Faulty Operation Modes

This section presents the 3-phase inverter associated with a motor in normal and faulty operation modes.

A. *Inverter operation*

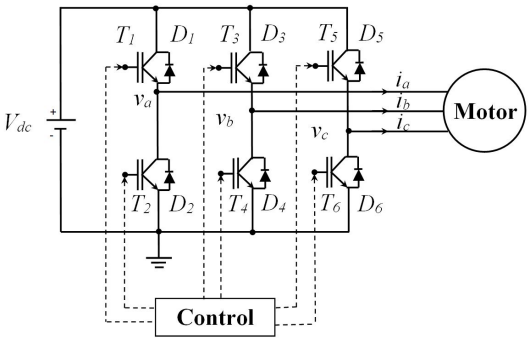

Fig. 1: 3-phase inverter driving a motor [4].

The considered system is a combination of a 3-phase inverter and a motor with the following specifications: star coupling for the stator with the isolated neutral, symmetric motor electrical circuit operating under open-loop control based on pulse width modulation (PWM). We assume that no fault occurs during the motor starting period. Each inverter leg is composed of two IGBTs and two inverse diodes as illustrated in Fig. 1.

TABLE I: Operation modes, diode states and electric potential of leg a.

	$i_a < 0$		$i_a > 0$	
	T_1 open	T_1 closed	T_1 open	T_1 closed
T_2 open	OC fault	normal or OC fault or SC fault	OC fault	normal or OC fault or SC fault
	D_1 closed D_2 open	D_1 closed D_2 open	D_1 open D_2 closed	D_1 open D_2 open
	$v_a = V_{dc}$	$v_a = V_{dc}$	$v_a = 0$	$v_a = V_{dc}$
T_2 closed	normal or OC fault or SC fault	SC fault	normal or OC fault or SC fault	SC fault
	D_1 open D_2 open		D_1 open D_2 closed	
	$v_a = 0$		$v_a = 0$	

Since the three legs of the inverter are symmetric, only the operation states of leg a is described in Table I. An inverter operation mode is defined as a time sequence of IGBT operation states. In the normal operation mode, T_1 and T_2 are alternatively open or closed with the PWM switching frequency. When IGBT T_1 or T_2 is closed all the time, the inverter is in SC fault mode, which is not considered in this work. When IGBT T_1 or T_2 is open all the time, the inverter is in OC fault mode, which will be investigated in the next subsection.

B. *Open-circuit fault analysis*

Fig. 2 illustrates the profiles of the three stator AC currents in steady-state where the system is in the normal mode before 0.40 s, and in the T_1 OC fault mode after 0.40 s.

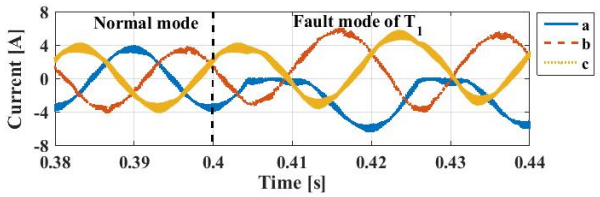

Fig. 2: Phase AC currents in the normal and T_1 fault modes.

The switching frequency of IGBTs is assumed to be much higher than the sinusoidal signal frequency. In the normal operation mode, when we generate the PWM signal to control the IGBTs based on three sinusoidal signals with frequency f and shifted by $2\pi/3$ between their phases, the three profiles of the stator currents are also sinusoidal with the same frequency and phase shifts at the steady state. Indeed, there is still the small oscillation in the current profiles because of IGBT switching (see Fig. 2).

The inverter is in T_1 (respectively T_2) OC fault mode if T_1 (respectively T_2) is open all the time while other IGBTs are still alternatively closed and open. In this case, if the current $i_a(t)$ is negative, the current profiles are still sinusoidal. It can be seen in Fig. 2 where the fault happens at 0.4 s. This is due to the fact that the electric potential profile of phase a, $v_a(t)$, does not change with respect to the normal mode according to Table I. However, if the current $i_a(t)$ is positive, the electric potential of phase a, $v_a(t)$, is always equal to zero, and the phase-a current, $i_a(t)$, reduces to zero quickly and stays like this for about half a period [9].

Thus, we can deduce an important characteristic of the stator currents in the faulty mode: the positive part of the phase-a current, $i_a(t)$, is "cut-off" when T_1 is faulty. Consequently, only the phase-a current is always negative during the T_1 fault mode. This results in the fact that the ratio between its average and the average of its absolute value on a fundamental signal period is equal to -1. Moreover, these ratios for the other phase currents are theoretically constant. Similarly, this observation can be easily extended to the fault cases of the other IGBTs. Hence, each mode can be represented by a vector constructed from these ratios. These presented fault characteristics will be exploited to formulate the feature variable in the next section.

III. Hybrid fault diagnosis method

In this section, a hybrid diagnosis method is presented which includes the following steps (as illustrated in Fig. 3): feature extraction, data clustering, labelling and fault detection and isolation.

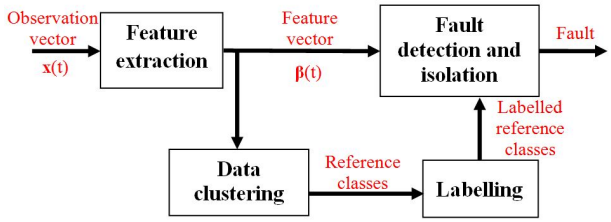

Fig. 3: Fault diagnosis algorithm.

A. *Feature extraction*

In this step, we focus on finding the feature vector which gathers all the feature variables. The linear space representing this vector is called feature space where feature vectors corresponding to different operation modes are located in different, distinguished regions in this space.

Let $\mathbf{x}(t)$, $\boldsymbol{\beta}(t)$ be, respectively, the observation and feature vectors at time instant $t = kt_s$, where t_s is the sampling time, and $k \in \mathbb{N}$ is the sampling time index. In our case, the measured variables are the 3-phase currents denoted by $i_a(t),\ i_b(t),\ i_c(t) \in \mathbb{R}$. Therefore, the observation vector is defined as:

$$\mathbf{x}(t) = \begin{bmatrix} i_a(t) & i_b(t) & i_c(t) \end{bmatrix}^T \in \mathbb{R}^3. \tag{1}$$

According to the faulty mode analysis in Section II, the feature vector is chosen as:

$$\boldsymbol{\beta}(t) = \begin{bmatrix} \beta_a(t) & \beta_b(t) & \beta_c(t) \end{bmatrix}^T \in \mathbb{R}^3, \tag{2a}$$

$$\text{with } \beta_l(t) = \frac{\sum_{k=0}^{N-1} i_l(t-kt_s)}{\sum_{k=0}^{N-1} |i_l(t-kt_s)|},\ l = a, b, c, \tag{2b}$$

where $N \in \mathbb{N}$ is the number of time samples on a fundamental signal period. The feature vector, $\boldsymbol{\beta}(t)$, will be used as the input to the following clustering procedure.

B. *Data clustering*

Here, we describe AUDyC, the algorithm chosen for data clustering, thanks to its on-line, adaptive and unsupervised learning capabilities [1], [2]. AUDyC automatically creates data classes in the feature space from the feature data. In our case, these classes represent the normal and single OC fault (i.e., a single transistor is faulty at a time) modes. Since each operation mode is ideally represented by a unique nominal feature vector, we consider a simplified formulation of AUDyC algorithm in this paper. This simplification is obtained by assuming that the data of each class follows a gaussian distribution around the nominal feature vector. Thus, a class is characterized by the mean vector and the covariance matrix. Class parameters are determined in the following 5 main procedures: the similarity verification, the creation, the adaptation, the fusion and the evaluation of classes, as illustrated in Fig. 4. These steps are performed whenever there is a new feature vector.

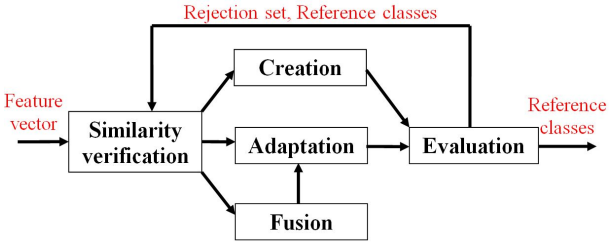

Fig. 4: AUDyC algorithm [2].

Similarity verification: This procedure finds the class to which the new feature vector, $\boldsymbol{\beta}(t)$, belongs, by quantifying similarities between this vector and existing classes based on membership functions defined as:

$$\mu_j(\boldsymbol{\beta}(t)) = \exp\left(-\frac{\tilde{\boldsymbol{\beta}}(t)^T \Sigma_j^{-1}(t-t_s)\tilde{\boldsymbol{\beta}}(t)}{2}\right), \tag{3}$$

where $\overline{\boldsymbol{\beta}}_j(t)$ and $\Sigma_j(t)$ are, respectively, the mean vector and the covariance matrix of class $\mathbb{C}_j$, and $\tilde{\boldsymbol{\beta}}(t) = \boldsymbol{\beta}(t) - \overline{\boldsymbol{\beta}}_j(t-t_s)$. Then, the values of these functions are compared to a threshold μ_{min} which leads to the definition of a similarity set $\mathbb{C}_{win}$:

$$\mathbb{C}_{win} = \{\mathbb{C}_j | \mu_j(\boldsymbol{\beta}(t)) \geq \mu_{min}\}. \tag{4}$$

Based on the cardinality of this set, we determine the next steps.

Creation: If $\text{card}\,(\mathbb{C}_{win}) = 0$, a new class $\mathbb{C}_j$ is created with the following parameters:

$$\begin{cases} \overline{\boldsymbol{\beta}}_j(t) &= \boldsymbol{\beta}(t), \\ \Sigma_j(t) &= \sigma^2 \mathbf{I}_3, \end{cases} \tag{5}$$

where $\mathbf{I}_3$ is the identity matrix of size 3, and $\sigma \in \mathbb{R}^+$ is a chosen parameter which determines the learning capacity of the created class at its first moment.

Adaptation: If $\text{card}\,(\mathbb{C}_{win}) = 1$, the similarity class $\mathbb{C}_j \in \mathbb{C}_{win}$ is adapted. Let $n_j(t) \in \mathbb{N}$ be the number of feature vectors belonging to $\mathbb{C}_j$ at time instant t. If $n_j(t-t_s) < N_{min}$, where N_{min} is a given threshold, the feature vector is stored in the memory of class $\mathbb{C}_j$. Moreover, the parameters of $\mathbb{C}_j$ are modified using the new feature vector:

$$\begin{cases} n_j(t) &= n_j(t-t_s) + 1, \\ \overline{\boldsymbol{\beta}}_j(t) &= \overline{\boldsymbol{\beta}}_j(t-t_s) + \dfrac{\tilde{\boldsymbol{\beta}}(t)}{n_j(t)}, \\ \Sigma_j(t) &= \Sigma_j(t-t_s). \end{cases} \tag{6}$$

If $N_{min} \leq n_j(t-t_s) < N_{max}$, where N_{max} is a given threshold, the feature vector is stored. $n_j(t)$ and $\overline{\boldsymbol{\beta}}_j(t)$ are modified according to the same formulas in (6), and $\Sigma_j(t)$ is given as:

$$\Sigma_j(t) = \frac{n_j(t)-2}{n_j(t)-1}\Sigma_j(t-t_s) + \frac{\tilde{\boldsymbol{\beta}}(t)\tilde{\boldsymbol{\beta}}(t)^T}{n_j(t)}. \tag{7}$$

If $n_j(t-t_s) = N_{max}$, the new feature vector is stored, and the oldest one is forgotten. Therefore, the prototype parameters are adapted by the following rules:

$$\begin{cases} n_j(t) &= N_{max}, \\ \overline{\boldsymbol{\beta}}_j(t) &= \overline{\boldsymbol{\beta}}_j(t-t_s) + \dfrac{\Delta\boldsymbol{\beta}(t)}{N_{max}} \begin{bmatrix} 1 \\ -1 \end{bmatrix}, \\ \Sigma_j(t) &= \Sigma_j(t-t_s) + \Delta\boldsymbol{\beta}(t)\mathbf{B}\Delta\boldsymbol{\beta}(t)^T, \end{cases} \tag{8}$$

with

$$\begin{cases} \Delta\boldsymbol{\beta}(t) = \begin{bmatrix} \boldsymbol{\beta}(t) - \overline{\boldsymbol{\beta}}_j(t-t_s) \\ \boldsymbol{\beta}(t - N_{max}t_s + t_s) - \overline{\boldsymbol{\beta}}_j(t-t_s) \end{bmatrix}^T, \\ \mathbf{B} = \dfrac{1}{N_{max}} \begin{bmatrix} 1 & \dfrac{1}{N_{max}-1} \\ \dfrac{1}{N_{max}-1} & -\dfrac{N_{max}+1}{N_{max}-1} \end{bmatrix}. \end{cases} \tag{9}$$

Fusion: When $\text{card}\,(\mathbb{C}_{win}) \geq 2$, if each two classes $\mathbb{C}_j, \mathbb{C}_m \in \mathbb{C}_{win}$ satisfy the condition:

$$tr\left(\Sigma_j(t)\Sigma_m^{-1}(t) + \Sigma_m(t)\Sigma_j^{-1}(t)\right) - 6 < \epsilon_f, \tag{10}$$

all the similarity classes are fused, where $tr(\mathbf{X})$ is the trace of matrix $\mathbf{X}$, ϵ_f is a given threshold. The classes are organized in the appearance order. The new class obtained by fusing two first classes is fused with the third class. The procedure is repeated until all the similarity classes are fused. Then, the parameters of the final fusion class is adapted to include the new feature vector. If (10) is not satisfied, only the parameters of the class with the highest value of the membership function in (3) is adapted with the new feature vector.

Evaluation: After every N_{min} time samples, a noisy cluster $\mathbb{C}_j$ is eliminated if:

$$\text{card}(\mathbb{C}_j) < N_{min}. \tag{11}$$

$\mathbb{C}_j$ is removed from the set of the reference classes, and all its feature vectors are stored in a rejection set for reuse in the next learning iteration (see Fig. 4).

AUDyC clusters feature data to different classes representing different system operation modes. These classes have no physical meaning, hence, it is necessary to determine their corresponding names in the following labelling procedure.

C. *Labelling*

Based on the physical knowledge available, conditions are formulated to determine the class names. In our case, we assume that there are 7 operation modes: normal mode and 6 single OC fault modes corresponding to the 6 IGBTs in the 3-phase inverter.

Let $\overline{\beta}_{a,j}$, $\overline{\beta}_{b,j}$, $\overline{\beta}_{c,j} \in \mathbb{R}$ be, respectively, the coordinates of the mean vector $\overline{\boldsymbol{\beta}}_j$ of class $\mathbb{C}_j$. From the analysis in the last paragraph of Section II, we notice that the feature variables defined by (2b) are close to zero in the normal mode and converge to 1 or -1 in the faulty modes. Thus, a labelling threshold ϵ_l is given to verify if the mean vectors of the modelled prototypes are close to these reference values. A class represents an operation mode if $\overline{\boldsymbol{\beta}}_j$ satisfies the corresponding conditions in Table II. If there is no satisfied condition, the class represents an unknown mode.

TABLE II: Labelling conditions.

Mode	Condition
Normal	$\left\lvert\overline{\boldsymbol{\beta}}_j\right\rvert < \sqrt{3}\epsilon_l$
Fault T_1	$-1-\epsilon_l < \overline{\beta}_{a,j} < -1+\epsilon_l$
Fault T_2	$1-\epsilon_l < \overline{\beta}_{a,j} < 1+\epsilon_l$
Fault T_3	$-1-\epsilon_l < \overline{\beta}_{b,j} < -1+\epsilon_l$
Fault T_4	$1-\epsilon_l < \overline{\beta}_{b,j} < 1+\epsilon_l$
Fault T_5	$-1-\epsilon_l < \overline{\beta}_{c,j} < -1+\epsilon_l$
Fault T_6	$1-\epsilon_l < \overline{\beta}_{c,j} < 1+\epsilon_l$

Based on these labels, we can determine the mode names of the new feature vectors in the following section.

D. *Fault detection and isolation*

This procedure concentrates on finding criteria which indicate the similarity of the new feature vector and the clustered classes. Using only the new feature vector for diagnosing the OC fault may cause false alarms due to two reasons: perturbations or temporary passage. The temporary passage implies that the feature vector may rapidly pass through a class which does not represent the actual operation mode. To deal with these false alarm causes, we consider a sequence of consecutive feature vectors, $\mathbb{B}(t) = \{\boldsymbol{\beta}(t - N_f t_s + t_s), \ldots, \boldsymbol{\beta}(t)\}$, where $N_f \in \mathbb{N}$ is a chosen parameter defining the width of the sequence. We find the reference class to which most of vectors of $\mathbb{B}(t)$ belong. Then, the number of vectors of $\mathbb{B}(t)$ belongs this class is used as the fault indicator.

Let $n_p(t) \in \mathbb{N}$ be the number of existing classes. We define the indication matrix $\mathbf{M}(t) \in \{0,1\}^{N_f \times n_p(t)}$ such that:

$$m_{kj}(t) = \begin{cases} 1, & \text{if } \mu_j(\boldsymbol{\beta}(t-kt_s+t_s)) = \\ & \quad \max_p \mu_p(\boldsymbol{\beta}(t-kt_s+t_s)) \geq \mu_f, \\ 0, & \text{if else,} \end{cases} \tag{12}$$

where $m_{kj}(t)$ is the element on the k^{th} row and j^{th} column of matrix $\mathbf{M}(t)$, $\mu_j(\boldsymbol{\beta}(t))$ is the membership function of class $\mathbb{C}_j$ defined in (3), μ_f is a given indication threshold. The fault indicator is the maximum absolute column sum norm of matrix $\mathbf{M}(t)$, that is:

$$I(t) = \max_j \sum_{k=1}^{N_f} |m_{kj}(t)|\,. \tag{13}$$

Let j_{max} be the index of the column whose absolute column sum is highest. The system operation is in the mode corresponding to class $\mathbb{C}_{j_{max}}$ if $I(t) \geq I_f$, where $I_f \in \mathbb{N}$ is a given fault threshold. Otherwise, the system is in an unknown faulty mode. The fault detection strongly depends on the parameters chosen for the AUDyC algorithm. Therefore, the detection time is not easy to be mathematically estimated.

The presented diagnosis procedure is validated using simulation and experiment data in the next section.

IV. Diagnosis results

Using the proposed method, this section presents the diagnosis results for the inverter single OC fault based on simulation and experiment data. In Scenario 1, simulation data are obtained using Simscape Electrical toolbox in Matlab. In Scenario 2, experimental data on a 5-phase inverter is provided by the L2EP laboratory in Lille, France. The properties of the data and the parameters of the diagnosis algorithm are presented in Table III. In the following result analysis, the mode flag is described by the natural variable $fault$. It is set to 0 if the operation mode is not detected.

TABLE III: Parameters for the data and the diagnosis algorithm.

Parameter	Unit	Scen. 1	Scen. 2
Data			
Signal frequency	[Hz]	50	50
Sample time t_s	[μs]	200	80
PWM switching frequency	[Hz]	5000	10000
AUDyC			
Class membership threshold μ_{min}	-	0.7	0.7
Initial covariance σ	-	0.8	0.8
Minimum class cardinality N_{min}	-	40	150
Maximum class cardinality N_{max}	-	100	250
Fusion threshold ϵ_f	-	3.2	3.2
Labelling			
Labelling threshold ϵ_l	-	0.1	0.1
Fault detection and isolation			
Indication threshold μ_f	-	0.8	0.8
Sliding window width N_f	-	50	150
Fault threshold I_f	-	30	130

A. *Scenario 1: Simulation data*

The normal mode and 6 alternative single OC fault modes are implemented as described in Table IV. The first row indicates the time durations of each mode. The third row indicates the corresponding reference values of the fault flag.

TABLE IV: Settings and detection times in Scenario 1.

Time [s]	0.2	0.1	0.1	0.1	0.1	0.1	0.1
Fault	None	T_1	T_2	T_3	T_4	T_5	T_6
$fault_{ref}$	1	2	3	4	5	6	7
Det. time [ms]		17.4	26.2	25.2	22.2	12.4	21.8

The profiles of the phase currents and of the feature variables are described in Fig. 5. This figure illustrates the remark in Section II.B: when an OC fault happens, the positive (or negative) part of the current in the corresponding leg is cut-off. It results in the -1 (or 1) value of the corresponding feature variable.

Fig. 6 describes the feature classes obtained using AUDyC corresponding to the operation modes. To verify if these classes characterize the operation modes in Scenario 1, we recall the conditions in Table II.

Fig. 7 and IV describes the diagnosed operation modes and the corresponding detection times. We see that all the operation modes are identified. The time duration of the mode diagnosis includes two periods. For example, we consider the time period from 0.2000 s to 0.2132 s. First of all, from 0.2000 s, the system operation is still in the normal mode though a fault happens. From 0.2132 s, an unknown operation mode is declared since the feature set, $\mathbb{B}(t)$, is not close to any class. Until 0.2174 s, Mode 2 is declared, and thus, the detection time is 0.0174s. The obtained detection times are short enough for turning off the system or reconfiguring the controller without the damage to the inverter and motor.

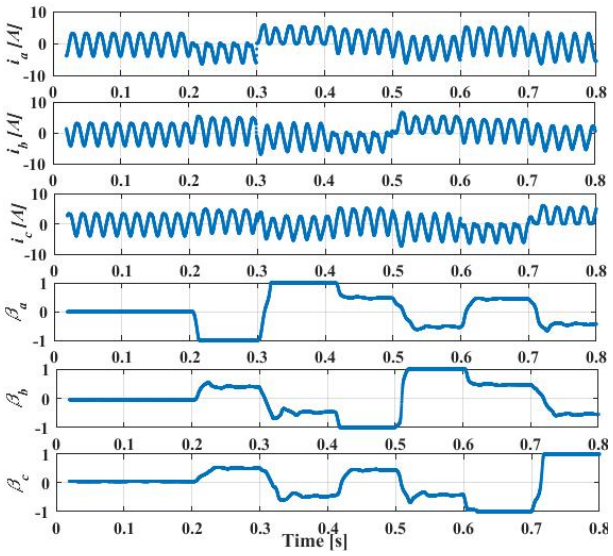

Fig. 5: Profiles of currents and of feature variables.

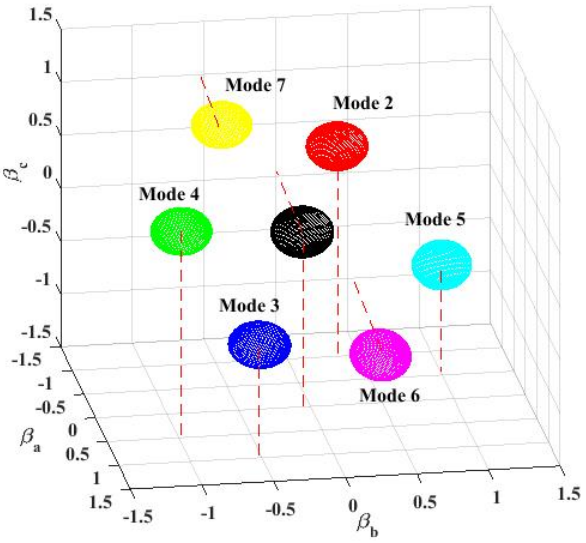

Fig. 6: Clustered classes in the feature space in Scenario 1.

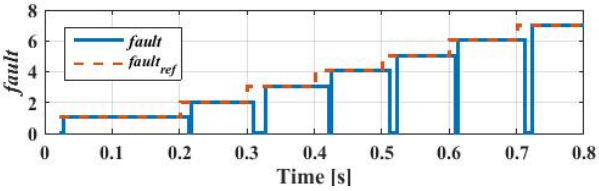

Fig. 7: Profiles of the fault flag in Scenario 1.

B. *Scenario 2: Experiment data*

Even though the paper focused on the 3-phase inverter, the procedure can be applied to 5-phase inverters with minimal changes as shown in this test case. The normal mode and 4 alternative single OC fault modes are implemented as described in Table V. The diagnosis results similar to one in Scenario 1 are illustrated in Fig. 8 and 9.

TABLE V: Settings and detection times in Scenario 2.

Time [s]	0.25	0.25	0.25	0.25	0.25
Fault	None	T_4	T_3	T_2	T_1
$fault_{ref}$	1	5	4	3	2
Det. time [ms]		22.88	36.64	27.20	30.32

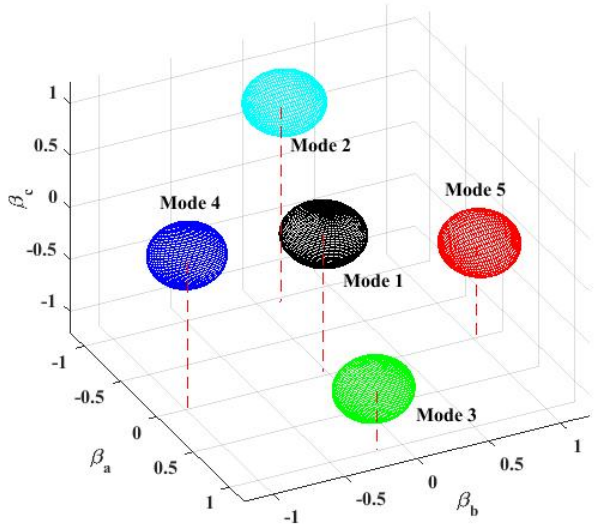

Fig. 8: Projection of clustered classes on the $\beta_a\beta_b\beta_c$ space in Scenario 2.

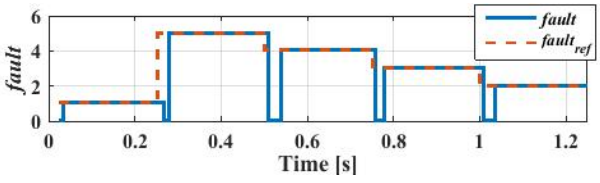

Fig. 9: Profiles of the fault flag in Scenario 2.

V. Conclusions

This paper presented a hybrid diagnosis approach for the single open-circuit faults in inverters. The approach consists of the following steps: feature extraction, data clustering, labelling and fault detection and isolation. The normalized DC current method is used to extract the features of different faulty operation modes based on the motor stator currents. In particular, the Auto-adaptive and Dynamical Clustering algorithm was employed for data clustering thanks to its on-line, adaptive and unsupervised learning capacities. Based on the obtained classes, we formulate the conditions for the labelling and fault detection and isolation. The approach was validated on simulation and experiment data. The short term future work concentrates on investigating the influence of the algorithm parameters on the detection time and making suggestions for choosing the ones yielding the smallest possible times. Moreover, the proposed approach would be compared with signal-based methods which is popularly used in the power electronic community.

Acknowledgement

This work has been achieved within the framework of the CE2I project (Convertisseur d'Energie Intégré Intelligent). CE2I is co-financed by European Union with the financial support of European Regional Development Fund (ERDF), the French State and the French Region of Hauts-de-France. The authors would like also to thank Eric Semail and Ngac Ky Nguyen from the L2EP laboratory in Lille (France) for providing the experimental data used in the second scenario.

References

[1] S. Lecoeuche, C. Lurette, and S. Lalot, "New supervision architecture based on on-line modelling of non-stationary data," *Neural Computing & Applications*, vol. 13, no. 4, pp. 323 – 338, December 2004.

[2] H. A. Boubacar, S. Lecoeuche, and S. Maouche, "Audyc neural network using a new gaussian densities merge mechanism," in *Adaptive and Natural Computing Algorithms*. Springer, 2005, pp. 155 – 158.

[3] M. Trabelsi, E. Semail, and N. K. Nguyen, "Experimental investigation of inverter open-circuit fault diagnosis for bi-harmonic five-phase permanent magnet drive," *IEEE Journal of Emerging and Selected Topics in Power Electronic*, vol. 6, no. 1, pp. 339 – 351, March 2018.

[4] B. Cai, Y. Zhao, H. Liu, , and M. Xie, "A data-driven fault diagnosis methodology in three-phase inverters for PMSM drive systems," *IEEE Transactions on Power Electronics*, vol. 32, no. 7, pp. 5590 – 5600, July 2017.

[5] Z. Gao, C. Cecati, and S. X. Ding, "A survey of fault diagnosis and fault-tolerant techniquespart II: Fault diagnosis with knowledge-based and hybrid/active approaches," *IEEE Transactions on Industrial Electronics*, vol. 62, no. 6, pp. 3768 – 3774, June 2015.

[6] J. Poon, P. Jain, I. C. Konstantakopoulos, C. Spanos, S. K. Panda, and S. R. Sanders, "Model-based fault detection and identification for switching power converters," *IEEE Transactions on Power Electronics*, vol. 32, no. 2, pp. 1419 – 1430, February 2017.

[7] N. S. Ahmad, A. R. Abdullah, and N. Bahari, "Open and short circuit switches fault detection of voltage source inverter using spectrogram," *Journal of International Conference on Electrical Machines and Systems*, vol. 3, no. 2, pp. 190 – 199, 2014.

[8] J. O. Estima and A. J. M. Cardoso, "A new algorithm for real-time multiple open-circuit fault diagnosis in voltage-fed PWM motor drives by the reference current errors," *IEEE Transactions on Industrial Electronics*, vol. 60, no. 8, pp. 3496 – 3505, August 2013.

[9] D.-E. Kim and D.-C. Lee, "Fault diagnosis of three-phase PWM inverters using wavelet and SVM," *Journal of Power Electronics*, vol. 9, no. 3, pp. 377 – 385, May 2009.

[10] C. Delpha, D. Diallo, H. A. Samrout, and N. Moubayed, "Multiple incipient fault diagnosis in three-phase electrical systems using multivariate statistical signal processing," *Engineering Applications of Artificial Intelligence*, vol. 73, pp. 68 – 79, 2018.

[11] J. F. Martins, V. Fernao-Pires, and A. J. Pires, "Unsupervised neural-network-based algorithm for an on-line diagnosis of three-phase induction motor stator fault," *IEEE Transactions on Industrial Electronics*, vol. 54, no. 1, pp. 259 – 264, February 2007.

[12] M. A. Masrur, Z. Chen, and Y. Murphey, "Intelligent diagnosis of open and short circuit faults in electric drive inverters for real-time applications," *IET Power Electronics*, vol. 3, no. 2, pp. 279 – 291, March 2010.

[13] L. Meng, P. Wang, Z. Liu, R. Qiu, L. Wang, and C. Xu, "Safety assessment for electrical motor drive system based on SOM neural network," *Mathematical Problems in Engineering*, vol. 2016, 2016, 8 pages.

[14] M. Talha, F. Asghar, and S. H. Kim, "A Matlab and Simulink based three-phase inverter fault diagnosis method using three-dimensional features," *International Journal of Fuzzy Logic and Intelligent Systems*, vol. 16, no. 3, pp. 173 – 180, September 2016.